J. Fluid Mech. (1990), vol. 212, pp. 65–80
Printed in Great Britain

Self-propulsion of asymmetrically vibrating bubbles

By T. BROOKE BENJAMIN[1] AND ALBERT T. ELLIS[2]
[1] Mathematical Institute, 24/29 St Giles, Oxford OX1 3LB, UK
[2] Institute for Nonlinear Science, Department of Applied Mechanics and Engineering Sciences, B-010, University of California, La Jolla, CA 92093, USA

(Received 30 June 1989)

The theory developed aims to explain erratic motions that have been observed experimentally to be performed by small bubbles in liquids irradiated by sound. An exact relation between dynamic and kinematic integral properties of any bubble is used as the basis for calculating the propulsive effects of deformations from spherical shape. The analysis deals first with arbitrary axisymmetric perturbations, such that the equation of the bubble's surface is representable in terms of zonal spherical harmonics, and then more general deformations are treated. It is shown that self-propulsion is accountable wholly to interactions of surface modes n and $n+1$ ($n = 2, 3, \ldots$). The resulting velocity $\boldsymbol{W}$ of the bubble's centroid is found to depend on the relative orientation of the interacting modes, $|\boldsymbol{W}|$ being greatest when they are coaxial but the direction of $\boldsymbol{W}$ having the more sensitive dependence. Supported by the theoretical results, an interpretation of the observed erratic motions is presented finally, and a few experimental observations are noted.

1. Introduction

The calculations to be presented were completed in the course of collaborative experimental and theoretical research on the behaviour of small gas bubbles in liquids subject to acoustic standing waves. The investigation as a whole which has explored a variety of phenomena will be reported in due course (Ellis & Benjamin 1990); but the present piece of theory deserves a separate account, having several points of incidental interest. Its main import is to account plausibly for a curious phenomenon first noticed by Gaines (1932), which has been reported by Kornfeld & Suvorov (1944) and several others since but has not until now been explained decisively.

In the original experiments, intense sound waves in water were generated by near-resonant longitudinal vibrations of a nickel tube, which were excited electronically by magnetostriction. In Kornfeld & Suvorov's experiments the frequency of the vibrations was about 7.5 kHz. When their amplitude was about 0.005 mm, tiny air bubbles were observed to form on the flat end of the tube and to move over the surface at a comparatively slow rate; but occasionally a few of the bubbles detached from the surface and rushed about rapidly within the liquid. Called 'dancing bubbles' by Gaines, they moved in zig-zag paths reminiscent of Brownian motion. When the amplitude was raised to about 0.01 mm or above, a whitish cloud was observed over the end of the vibrating tube, consisting apparently of many tiny, rapidly moving bubbles. Kornfeld & Suvorov presented photographs of bubbles attached to the end of the vibrating tube, which show them to oscillate in various regular patterns of deformation, depending on bubble size. Taken with spark illumination, other photographs of detached, vigorously dancing bubbles show them to execute wild variations in shape and sometimes disintegrate.

The parametric excitation of shape oscillations in free bubbles pulsating radially in a sound field was proposed by Benjamin & Strasberg (1958) and Strasberg & Benjamin (1958; see also Benjamin 1964) as a cause of the erratic motions observed. This example of parametric excitation, such that the shape oscillations have half the frequency of the sound, is explainable by the linearized equation for the time-dependent amplitude of asymmetric perturbations relative to a pulsating spherical bubble, which equation is reducible to Mathieu's equation approximately and was first derived by Plesset & Mitchell (1956; see also Hsieh & Plesset 1961). The precise reason why bubbles so excited may be propelled along an erratic path has not yet been exhibited, however, and the principal aim of this paper is to answer the outstanding question.

The mechanism now at issue was virtually anticipated by Saffman (1967), who showed by an example that a deforming, nearly spherical body can propel itself in an infinite perfect fluid. Saffman deserves full credit for the idea to be re-examined here; but the specific results given by him for the relevant example appear to be in error, even to the extent of predicting a propulsive effect with the wrong sign. His account was drastically abbreviated, merely quoting the results of a 'straightforward but tedious calculation'; and a reappraisal in more detail than given by him is warranted. The reasoning needed to secure the prediction of self-propulsion due to a general form of deformation is delicate and demands a fuller account.

The method to be adopted differs from Saffman's although it is consistent with the principles expounded in his paper. The analysis will be based on an exact integral relation derived in a recent paper about Hamiltonian theory for motions of bubbles in an infinite perfect liquid (Benjamin 1987). Introducing notation required to express this relation, let ϕ denote the velocity potential for the motion of the liquid surrounding a simply connected bubble, and let Φ denote the evaluation of ϕ at the surface S of the bubble. The liquid is taken to have unit density and to be stationary at infinity. Being a harmonic function of position $\boldsymbol{x}$ in the exterior domain, ϕ is for any S uniquely determined by Φ and the asymptotic condition $|\nabla\phi| \rightarrow 0$ as $|\boldsymbol{x}| \rightarrow \infty$. Then the linear Kelvin impulse of the motion (Lamb 1932, §§120 and 121) is defined by

$$\boldsymbol{I} = -\int_S \Phi \boldsymbol{n}\, \mathrm{d}s, \tag{1.1}$$

where $\boldsymbol{n}$ is the unit normal to S directed into the liquid. In the absence of external forces such as gravity and on the assumption that the interior of the bubble has zero inertia, the vector $\boldsymbol{I}$ is an invariant of the motion; and for present purposes attention can be confined to the case $\boldsymbol{I} = 0$.

In terms of spherical coordinates (r, θ, ψ), the asymptotic form of the velocity potential for $r \rightarrow \infty$ is in general

$$\phi = \frac{M}{r} + \frac{1}{r^2}(A_1 \cos\theta + A_2 \sin\theta\cos\psi + A_3 \sin\theta \sin\psi) + O\left(\frac{1}{r^3}\right), \tag{1.2}$$

where the monopole coefficient M and dipole coefficients A_i respective to orthogonal directions $i = 1, 2, 3$ are functions of time t alone. Finally, we introduce the vector

$$\boldsymbol{C} = \int_V \boldsymbol{x}\, \mathrm{d}v = \bar{\boldsymbol{x}}\mathscr{V}. \tag{1.3}$$

Here V denotes the space constituting the interior of the bubble, $\mathrm{d}v$ represents the element of volume (i.e. $r^2 \sin\theta\, \mathrm{d}r\, \mathrm{d}\theta\, \mathrm{d}\psi$), and $\mathscr{V}$ is the volume of V. Thus $\bar{\boldsymbol{x}}$ is the position of the bubble's centroid.

The general relation needing to be recalled is that, for all time t,

$$I_i + \frac{\mathrm{d}C_i}{\mathrm{d}t} + 4\pi A_i = 0 \quad (i = 1, 2, 3) \tag{1.4}$$

(Benjamin 1987, equation (2.18)). In the cited paper the three identities (1.4) were shown to follow, according to a version of Noether's theorem, from the Gallilean invariance of the hydrodynamic problem formulated as a Hamiltonian system; and the results (1.4) are confirmable otherwise as follows. With reference to the harmonic functions ϕ and each x_i, Green's theorem shows that the surface integral of $x_i\, \partial\phi/\partial n - \phi\, \partial x_i/\partial n$ over S equals the same integral over a sphere of radius R enclosing the bubble. Noting that $\partial x_i/\partial n = n_i$ and writing $\Phi_{(n)}$ for $\partial\phi/\partial n$ on S (cf. Benjamin 1987, p. 351), we therefore have

$$\int_S (x_i \Phi_{(n)} - \Phi n_i)\, \mathrm{d}s = \int_0^{2\pi} \int_0^{\pi} (x_i \phi_r - n_i \phi)_{r=R} R^2 \sin\theta\, \mathrm{d}\theta\, \mathrm{d}\psi. \tag{1.5}$$

The second integral on the left of this equality is I_i by the definition (1.1), and the first integral is evidently $\mathrm{d}C_i/\mathrm{d}t$. In the limit $R \to \infty$, the sum of the integrals on the right is found to be $-4\pi A_i$; and thus the relation (1.4) is confirmed. It should be acknowledged that (1.4) generalizes a well known result for *rigid* bodies translating in a perfect liquid (cf. Batchelor 1967, p. 401, eqn. (6.4.8); Lighthill 1978, pp. 38, 39). In the absence of external forces (1.4) holds for all t irrespective of changes in shape or volume.

In §§3 and 4 this relation will be used to calculate the axial velocity $\mathrm{d}\bar{x}_1/\mathrm{d}t$ enforced by time-dependent deformations of a bubble that remains symmetric about the x_1-axis, its surface being representable by series of zonal harmonics. In §5 the analysis will be extended to deformations of more general shape; and in §6 the theoretical results will serve to explain the observed erratic motions of small bubbles in sound fields. A sample of our experimental results is included finally in §6. The use of (1.4) explifies the advantages of exact, generalized integral properties as predictors of second-order quantities such as $\mathrm{d}\bar{x}_1/\mathrm{d}t$: the results are obtained decisively without need to approximate the nonlinear kinematic and dynamic boundary conditions at S to the same order. A comparably advantageous use of another integral relation for the motions of bubbles, a virial equation, was presented in a recent paper (Benjamin 1989).

2. First-order and second-order perturbations

We focus attention first on axisymmetric perturbations about a sphere of radius a, but we shall show in §5 how the results can be extended to more general perturbations of shape. In terms of spherical coordinates (r, θ, ψ) the surface S of the simply connected bubble is taken to be described by the equation

$$r = a\left\{1 + \epsilon_0 + \epsilon_1 \mu + \sum_{n=2}^{\infty} \epsilon_n P_n(\mu)\right\}, \tag{2.1}$$

in which $\mu = \cos\theta$ and P_n is the Legendre polynomial of order n ($P_0(\mu) = 1$, $P_1(\mu) = \mu$). The coefficients ϵ_n ($n = 0, 1, 2, \ldots$) are functions of t alone; and because the set $\{P_n\}_{n=0}^{\infty}$ of orthogonal polynomials is complete on $[-1, 1]$, equation (2.1) represents an arbitrary time-dependent surface that remains axisymmetric. The ϵ_n with $n \geqslant 2$ are taken to be $O(\epsilon)$, where ϵ is a representative small value, but ϵ_0 and ϵ_1 are for now taken to be $O(\epsilon^2)$. Generalizations relaxing these temporary assumptions will be explained in §6.

A corresponding expression for the velocity potential is

$$\phi = -\frac{Ba^3}{r} - \frac{Aa^4\mu}{r^2} - \sum_{n=2}^{\infty} \frac{a^{n+3}\{\dot{\epsilon}_n + O(\epsilon^2)\}P_n(\mu)}{(n+1)\,r^{n+1}}, \tag{2.2}$$

where B and A are $O(\epsilon^2)$. Note that consequently this expression satisfies to $O(\epsilon)$ the kinematic condition applying at the surface S described by (2.1) (see (4.3) below). Although B and A are of course related to ϵ_0 and ϵ_1, there will be no need at present to evaluate B, ϵ_0 and ϵ_1. The object is to find A, which is identifiable with $-A_1/a^4$ in (1.4), and this object is achievable directly from the condition that the axial component of Kelvin impulse should be zero, say $I_1 = 0$. (Needless to say, the axial symmetry implies $I_i = 0$ for $i = 2, 3$.) For the present purpose, use of this integral condition obviates the need to satisfy the kinematic and dynamic boundary conditions explicitly to $O(\epsilon^2)$.

For substitution in the integrand of I_1, it appears at once from (2.2) that

$$-\Phi/a^2 = B + A\mu + \sum_{n=2}^{\infty} (n+1)^{-1}\{\dot{\epsilon}_n + O(\epsilon^2)\}P_n(\mu) - \sum_{n=2}^{\infty}\sum_{m=2}^{\infty} \dot{\epsilon}_n\,\epsilon_m\,P_n(\mu)\,P_m(\mu) + O(\epsilon^3). \tag{2.3}$$

Next, because to $O(\epsilon)$ the unit normal $\boldsymbol{n}$ to S is $(1, -\eta_\theta, 0)$, where $\eta = r/a$ as given by (2.1), its axial component is

$$\begin{aligned} n_1 &= \cos\theta + \eta_\theta \sin\theta \\ &= \mu - \sum_{n=2}^{\infty} \epsilon_n (1-\mu^2)\,P_n'(\mu) + O(\epsilon^2). \end{aligned} \tag{2.4}$$

Finally, the element of surface area is noted to be

$$\begin{aligned} \mathrm{d}s &= 2\pi r^2 \sin\theta\,\mathrm{d}\theta \\ &= -2\pi a^2\left\{1 + 2\sum_{n=2}^{\infty} \epsilon_n\,P_n(\mu) + O(\epsilon^2)\right\}\mathrm{d}\mu. \end{aligned} \tag{2.5}$$

Expressing the assumption that no external force acts on the bubble, we have

$$I_1 = -\int_S \Phi n_1\,\mathrm{d}s = 0 \tag{2.6}$$

for all t. Upon substitution of (2.3)–(2.5) in this integral, all terms of first order in ϵ are seen to cancel because $P_n(\mu)$ with $n \geqslant 2$ is orthogonal to $\mu = P_1(\mu)$ on $[-1, 1]$. To $O(\epsilon^2)$ the result obtained from (2.6) is that

$$\tfrac{2}{3}A = \sum_{n=2}^{\infty}\sum_{m=2}^{\infty} C_{n,m}\,\dot{\epsilon}_n\,\epsilon_m, \tag{2.7}$$

where

$$C_{n,m} = \int_{-1}^{1}\left\{\left(\frac{n-1}{n+1}\right)\mu P_n(\mu)\,P_m(\mu) + \frac{1}{n+1}(1-\mu^2)\,P_n(\mu)\,P_m'(\mu)\right\}\mathrm{d}\mu. \tag{2.8}$$

Having been derived with comparative ease by use of (2.6), the result (2.7) for A to $O(\epsilon^2)$ might otherwise be obtained by development of second-order approximations to the kinematic and dynamic boundary conditions. The latter method would be necessary if the interrelations among all the $\epsilon_i(t)$ including $\epsilon_0(t)$ and $\epsilon_1(t)$ were to be found; but this more complicated task can be avoided without loss at present. Equations (1.4) and (2.6) capture the relevant dynamical principles exactly, and our second-order approximations to these equations will suffice to account for the phenomenon principally in question.

3. Evaluation of coefficients

To evaluate the numbers $C_{n,m}$ in (2.7), consider the recurrence formulae for Legendre polynomials

$$\mu P_n = \frac{1}{2n+1}\{(n+1)P_{n+1} + nP_{n-1}\},$$

$$(1-\mu^2)P'_n = n(P_{n-1} - \mu P_n),$$

together with their orthogonality and normalization

$$\int_{-1}^{1} P_n(\mu)\,P_m(\mu)\,\mathrm{d}\mu = \begin{cases} 0 & \text{if } m \neq n, \\ \dfrac{2}{2n+1} & \text{if } m = n \end{cases}$$

(cf. Whittaker & Watson 1927, §§15.14, 15.21; Jeffreys & Jeffreys 1956, §§24.07, 24.10). It is at once seen that $C_{n,m} = 0$ unless $m = n \pm 1$; and moreover the second recurrence formula shows that $C_{n,n-1} = 0$, because with $m = n-1$ the two non-zero integrals composing the right-hand side of (2.8) cancel. In the evaluation of $C_{n,n+1}$, factors $n(n+1)(2n+1)$ are found to cancel between the numerator and denominator, and the result is

$$C_{n,n+1} = \frac{2}{2n+3} \quad (n = 2, 3, \ldots). \tag{3.1}$$

Hence (2.7) reduces to

$$A = \sum_{n=2}^{\infty} \frac{3}{2n+3}\dot{\epsilon}_n \epsilon_{n+1}. \tag{3.2}$$

Recalling that $I_1 = 0$ and $A_1 = -a^4 A$ in (1.4), and writing

$$\mathrm{d}C_1/\mathrm{d}t = \tfrac{4}{3}\pi a^3 W_1,$$

we may conclude from (1.4) and (3.2) that

$$W_1 = \sum_{n=2}^{\infty} \frac{9a}{2n+3}\dot{\epsilon}_n \epsilon_{n+1} + O(\epsilon^3). \tag{3.3}$$

For example, if only ϵ_2 and ϵ_3 are non-zero, (3.3) shows that

$$W_1 = \tfrac{9}{7}a\dot{\epsilon}_2 \epsilon_3 + O(\epsilon^3). \tag{3.4}$$

[This result appears irreconcilable with the result given by Saffman (1967, pp. 388, 389). He dealt with the case of a deformable, nearly spherical body with density equal to that of the surrounding liquid; but his result (15) is immediately adaptable to the present case of a deforming bubble. (Note that the second 2 in the factor on the right-hand side of his (15) is evidently a misprint; by comparison with (16) it should be 3.) For a bubble his result (16) becomes $W_1 = \frac{9}{7}a(3\epsilon_2\dot{\epsilon}_3 - 2\dot{\epsilon}_2\epsilon_3) + O(\epsilon^3)$, which is incompatible with our (3.4) above.]

4. Alternative derivation

A check on the crucial result (3.3) is provided by the following argument. Suppose that the centroid of the deforming axisymmetric bubble remains at the origin, so that $dC_1/dt = 0$ in (1.4). To ensure this property, fictitious external forces need to be applied to the surface S of the bubble, generating an axial Kelvin impulse which (1.4) shows to be $\tilde{I}_1 = -4\pi\tilde{A}_1$. Thus a calculation of $\tilde{A}_1$, namely the value of A_1 subject to the constraint $C_1 = 0$, will reveal the net axial impulse that the external forces must deliver in order to arrest movement of the bubble's centroid. Hence the velocity W_1 of the centroid in the absence of external forces can be inferred by d'Alembert's principle.

According to (2.1), the constraint

$$C_1 = 2\pi a^4 \int_{-1}^{1} [1+\eta(\mu)]^4 \mu \, d\mu = 0$$

is found to require that

$$\epsilon_1 = -\sum_{n=2}^{\infty}\sum_{m=2}^{\infty} D_{n,m}\,\epsilon_n\,\epsilon_m + O(\epsilon^3) \tag{4.1}$$

with

$$D_{n,m} = \frac{9}{2}\int_{-1}^{1} P_n(\mu)\,P_m(\mu)\,\mu\,d\mu. \tag{4.2}$$

Note that $D_{n,m} = 0$ unless $m = n \pm 1$. When only ϵ_2 and ϵ_3 are non-zero, for example, (4.1) and (4.2) give $\epsilon_1 = -(27/35)\,\epsilon_2\,\epsilon_3$ (cf. Saffman 1967, (13)).

Now consider the kinematic condition at the bubble's surface S. To second order in ϵ this condition is expressed by

$$\eta_t + a^{-2}(1-\mu^2)\,\eta_\mu\,\phi_\mu(a,\mu) = a^{-1}\phi_r(a,\mu) + \phi_{rr}(a,\mu)\,\eta. \tag{4.3}$$

Substituting for η from (2.1) and for ϕ from (2.2), then multiplying each term by μ and integrating over $[-1, 1]$, we deduce that

$$\tilde{A} = \tfrac{1}{2}\dot{\epsilon}_1 + \sum_{n=2}^{\infty}\sum_{m=2}^{\infty} E_{n,m}\,\dot{\epsilon}_n\,\epsilon_m + O(\epsilon^3) \tag{4.4}$$

with

$$E_{n,m} = \frac{3}{4}\int_{-1}^{1}\left\{(n+2)\,P_n(\mu)\,P_m(\mu) - \frac{1}{n+1}(1-\mu^2)\,P_n'(\mu)\,P_m'(\mu)\right\}\mu\,d\mu. \tag{4.5}$$

Note too that $E_{n,m} = 0$ unless $m = n \pm 1$.

From the properties of P_n recalled at the start of §3, it is further found that

$$\tfrac{1}{2}D_{n,n+1} = \frac{9(n+1)}{2(2n+1)(2n+3)}, \quad E_{n,n+1} = \frac{3(n+2)}{2(2n+1)(2n+3)},$$

$$\tfrac{1}{2}D_{n,n-1} = E_{n,n-1} = \frac{9n}{2(2n-1)(2n+1)}.$$

Hence the combination of (4.1) and (4.4) proves that

$$\tilde{A} = -\sum_{n=2}^{\infty} \frac{3}{2(2n+3)} \dot{\epsilon}_n \epsilon_{n+1} + O(\epsilon^3). \tag{4.6}$$

Thus $\tilde{A}$ is $-\frac{1}{2}$ times A given by (3.2). But the two results are in fact equivalent. Recall that the second-order axial impulse imparted to the liquid by the external forces needed to keep $C_1 = 0$ is $\tilde{I}_1 = -4\pi\tilde{A}_1 = 4\pi a^4\tilde{A}$, which is negative if A given by (3.2) is positive. According to d'Alembert's principle, the centroid will move in the direction opposite to that of $\tilde{I}_1$ when external forces are absent; and moreover the velocity W_1 of the centroid will then be given to second order by $\frac{2}{3}\pi a^3 W_1 = -\tilde{I}_1$, because to zeroth order the virtual mass of the bubble is $\frac{2}{3}\pi a^3$ (Lamb 1932, p. 124). It follows that $W_1 = -6a\tilde{A}$, whence (4.6) reconfirms the result (3.3).

5. Shape perturbations that are not axisymmetric

Plainly, as the hydrodynamic problem has the $O(3)$ symmetry group, the propulsive effect expressed by (3.3) is the same in any direction about which interacting surface modes n and $n+1$ are both axisymmetric. The condition of coaligned axial symmetry is an arbitrary simplification, however, having no evident physical cause; and it is highly pertinent to the interpretation given later that we should inquire into the effects of departures from this special condition.

To represent more general deformations of the sphere, the expansion (2.1) has to include terms in $P_n^k(\mu)(\cos k\psi, \sin k\psi)$, with summation over $k = 1, 2, \ldots, n$ as well as n. A calculation of the second-order dipole coefficients A_i subject to $I_i = 0$ ($i = 1, 2, 3$) can proceed by an obvious extension of the procedure in §§2 and 3, using recurrence formulae and integral properties for the orthogonal sets of associated Legendre functions $\{P_n^k(\mu)\}_{n=1}^{\infty}$. But the calculation is complicated, and little of interest is easily revealed by it. The following comparatively simple argument suffices to demonstrate the relocation and diminution of propulsive effects when interacting surface modes cease to be coaxial.

In the equation for S generalizing (2.1), suppose that the terms $O(\epsilon)$ include a mode $n+1$ that is symmetric about the axis from the origin to the point $(\theta, \psi) = (0, 0)$ on the unperturbed sphere, and also include a mode n that is symmetric about the axis through (θ', ψ') where $\theta' \neq 0$. Thus $\eta(\theta, \psi)$ includes the sum of $\epsilon_{n+1}P_{n+1}(\mu) = \epsilon_{n+1}P_{n+1}(\cos\theta)$ and $\epsilon_n P_n(\cos\gamma)$, where

$$\cos\gamma = \cos\theta\cos\theta' + \sin\theta\sin\theta'\cos(\psi - \psi').$$

Our object is to calculate the direction and magnitude of the contribution by these two terms to the second-order vector $\boldsymbol{W} = \mathrm{d}\bar{\boldsymbol{x}}/\mathrm{d}t$, which we know to be given by (3.3) in the case $\theta' = 0$.

The addition theorem for spherical harmonics is that

$$P_n(\cos\gamma) = P_n(\cos\theta)P_n(\cos\theta') + 2\sum_{k=1}^{n} \frac{(n-k)!}{(n+k)!} P_n^k(\cos\theta)P_n^k(\cos\theta')\cos k(\psi - \psi') \tag{5.1}$$

(Whittaker & Watson, 1927, p. 345; Jeffreys & Jeffreys 1956, §24.13). Retracing the steps whereby the expression (3.3) for W_1 was derived in §§2 and 3, one notices from (5.1) that in the present case no term of the summation over k contributes to W_1, because each prospective contribution to the second-order terms in the result for A_1

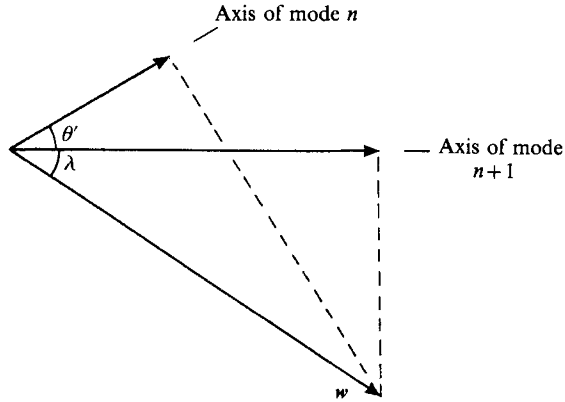

FIGURE 1. Deposition of scaled velocity $\boldsymbol{w}$ of propulsion in meridional plane common to mode $n+1$ with axis $\theta = 0$ and mode n with axis $\theta = \theta'$.

deriving from (2.6) is cancelled by integration with respect to ψ over $[0, 2\pi]$. From (5.1), moreover, the result for A_1 and hence W_1 is evidently the same as before except that ϵ_n is replaced by $\epsilon_n P_n(\cos\theta')$. Thus, writing $\cos\theta' = \mu'$, we infer the result

$$W_1(\mu') = W_1(1) P_n(\mu'), \tag{5.2}$$

in which according to (3.3)

$$W_1(1) = \frac{9a}{2n+3} \dot{\epsilon}_n \epsilon_{n+1}.$$

As before, because $C_{n,n-1} = 0$ for all n, no term in $\epsilon_n \dot{\epsilon}_{n+1}$ is presented in (5.2). It also appears from the properties of $C_{n,m}$ noted in §3 that, when $\eta(\theta, \psi)$ includes any number of modes $n = 2, 3, \ldots$ composed in pairs as at present, each with a respective value of μ', the result (5.2) is generalized by summation over n.

In particular, when the orientations of the modes n and $n+1$ in the present example are exchanged, the mode n being then symmetric about the original axis $\theta = 0$, the corresponding result is

$$W_1(\mu') = W_1(1) P_{n+1}(\mu'). \tag{5.3}$$

Equivalently, (5.3) is the component of $\boldsymbol{W}$ in the direction of the axis through (θ', ψ') in the present example. The facts implied by (5.2) and (5.3) are illustrated in figure 1, which shows how the vector $\boldsymbol{w} = \boldsymbol{W}/W_1(1)$ may be calculated.

Obviously $\boldsymbol{w}$ lies in the plane $\psi = \psi'$ through the origin, and so henceforth we can suppose $\psi' = 0$ without loss of generality. Let $\theta = -\lambda$ give the direction of $\boldsymbol{w}$ in this plane. Figure 1 shows that

$$\left.\begin{aligned} w_1 = |\boldsymbol{w}| \cos\lambda &= P_n(\mu') \\ \text{and} \qquad |\boldsymbol{w}| \cos(\lambda + \theta') &= P_{n+1}(\mu'). \end{aligned}\right\} \tag{5.4}$$

There follows directly

$$\tan\lambda = \frac{1}{(1+\mu'^2)^{\frac{1}{2}}} \left\{ \mu' - \frac{P_{n+1}(\mu')}{P_n(\mu')} \right\}, \tag{5.5}$$

whence λ can be calculated and $|\boldsymbol{w}|$ is then given by $P_n(\mu')(1+\tan^2\lambda)^{\frac{1}{2}}$. Note that λ passes through 90° (or odd multiple of 90°), and the radical just written changes sign, as μ' passes through a zero of P_n.

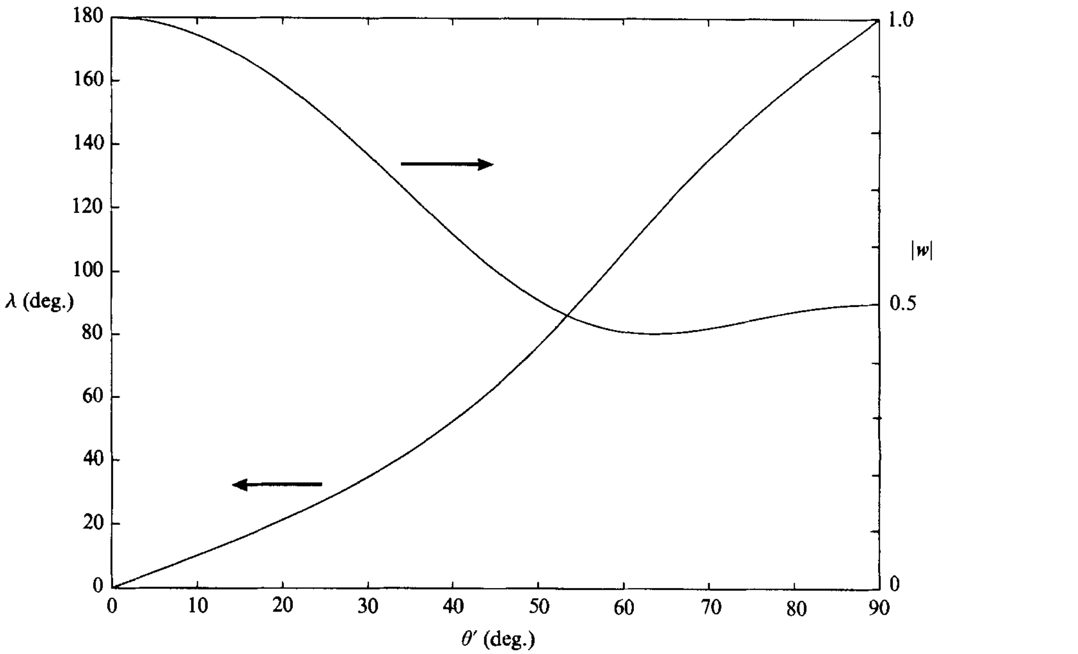

FIGURE 2. Values of λ (degrees) and $|\boldsymbol{w}|$ plotted against θ' (degrees), giving direction $\theta = -\lambda$ and magnitude of scaled velocity $\boldsymbol{w}$ of propulsion due to interaction between mode 3 with axis $\theta = 0$ and mode 2 with axis $\theta = \theta'$.

The result (5.5) may be derived alternatively by finding the dipole coefficient A_2, and hence w_2 according to (1.4), respective to the direction $(\frac{1}{2}\pi, 0)$ that is perpendicular to the axis of the mode $n+1$ in the meridional plane $\psi = 0$ shared by both modes. It appears from (5.1) that, in the calculation of A_2 to second order from the condition $I_2 = 0$, the only contribution to the coefficient of $\dot{\epsilon}_n \epsilon_{n+1}$ arises from the first term ($k = 1$) in the summation over k. Passing over the details, we quote the outcome

$$w_2 = -\frac{P_n^1(\mu')}{(1+n)} = -\frac{1}{(1-\mu'^2)^{\frac{1}{2}}}\{\mu P_n(\mu') - P_{n+1}(\mu')\},$$

which agrees with (5.4) and (5.5).

In the case $n = 2$, the result (5.5) reduces to

$$\tan\lambda = \frac{2\mu'(1-\mu'^2)^{\frac{1}{2}}}{3\mu'^2 - 1} = \frac{2\sin 2\theta'}{1+3\cos 2\theta'}. \tag{5.6}$$

Values of λ and $|\boldsymbol{w}|$ calculated from (5.6) and $|\boldsymbol{w}| = \frac{1}{2}(3\mu'^2-1)/\cos\lambda = \frac{1}{2}(5\mu'^4 - 2\mu'^2 + 1)^{\frac{1}{2}}$ are plotted against θ' between 0 and 90° in figure 2. It may be seen that as θ' increases from 0, at which $\lambda = 0$ and $|\boldsymbol{w}| = 1$, the angle λ of the vector $\boldsymbol{w}$ steadily increases while its magnitude $|\boldsymbol{w}|$ first decreases, then passes through a minimum value $1/\surd 5 = 0.44721$ and increases to the value 0.5 at $\theta' = 90°$. Note also that $\lambda = 180°$ at $\theta' = 90°$. Thus the direction of the propulsive effect is reversed, and its magnitude halved, when the axes of the modes $n = 2$ and 3 are changed from alignment to being orthogonal.

Both these conclusions can be expected. Consider how the added-mass coefficients for an ellipsoid of revolution vary as the eccentricity e of the meridian is varied near to zero. When $e > 0$ and the ellipsoid is prolate, the added-mass coefficient for axial motion is decreased from $\frac{2}{3}\pi a^3$ and that for sideways motion is increased from $\frac{2}{3}\pi a^3$. The direction of the changes is reversed when $e < 0$ and the ellipsoid is oblate. Moreover, the rate at which the first (axial) coefficient varies with e at $e = 0$ is found to be in magnitude *twice* that for the second (sideways) coefficient (cf. Lamb 1932, §§114, 373; Milne-Thomson 1968, §16.54; Kochin, Kibel & Roze 1964, §7.8, figures 150, 152). For small ϵ_2, the mode of deformation described by the zonal harmonic $P_2(\mu)$ in (2.1) is ellipsoidal; and the propulsive effect of interactions between modes 2 and 3 in a deforming bubble is accountable to variations in added mass that are out of phase with departures from fore-and-aft symmetry (due to the mode with $n = 3$; cf. Saffman 1967, p. 389). The two facts noted at the end of the last paragraph are thus explained.

Regarding figure 2, note finally how λ and $|\boldsymbol{w}|$ vary with θ' outside the range [0, 90°]. As is geometrically obvious in the example, λ is an odd function and $|\boldsymbol{w}|$ an even function of θ'. Also $|\boldsymbol{w}|$ is an even and $\lambda - 180°$ an odd function of $\theta' - 90°$.

6. Discussion

Consider the situation when just two aligned modes n and $n+1$ are excited parametrically into vibrations at frequency ω. According to (3.3), the centroid of the bubble then acquires a mean axial velocity $\overline{W}_1$ which is non-zero unless ϵ_n and ϵ_{n+1} are in phase. Writing $\epsilon_n = \hat{\epsilon}_n \sin(\omega t + \alpha)$ and $\epsilon_{n+1} = \hat{\epsilon}_{n+1}\cos(\omega t + \beta)$, we have in general

$$\overline{W}_1 = \frac{9}{2(2n+3)}\omega a \hat{\epsilon}_n \hat{\epsilon}_{n+1} \cos(\alpha - \beta) + O(\epsilon^3). \tag{6.1}$$

Furthermore, when the axes of the two modes cease to be aligned, the calculations in §5 show that the vector mean velocity $\overline{\boldsymbol{W}}$ of the centroid diminishes in magnitude from the value (6.1), although at most to only about 50%; and the direction of $\overline{\boldsymbol{W}}$ is remarkably sensitive to the angle θ' between the axes. The rate of dependence $|\mathrm{d}\lambda/\mathrm{d}\theta'|$ varies between about 1 and 3 in the case $n = 2$ illustrated by figure 2, and it increases with $n > 2$.

Figure 3(*a*) shows the shapes of a bubble at four successive stages in the cycle where interaction between modes 2 and 3 is producing maximum propulsive effect (i.e. $\alpha = \beta$, $\theta' = 0$). Figure 3(*b*) shows the corresponding shapes when $\theta' = 54.74°$ (so that $P_2(\mu') = 0$) and consequently $\overline{\boldsymbol{W}}$ is perpendicular to the axis of the mode 3.

Before highlighting the explanation for the observed erratic motions, we should note two important refinements of the foregoing theory.

Relaxation of assumption $\epsilon_1 = O(\epsilon^2)$

If $\overline{W}_1 \neq 0$ in the case of time-periodic deformations symmetric about the axis $\theta = 0$, the coefficient ϵ_1 in (2.1) will eventually cease to have the order of smallness $O(\epsilon^2)$ formally presumed for it in our analysis, which conveniently took the origin $r = 0$ to be fixed. But this formal limitation is obviated simply by redefining the origin to move with velocity $\overline{W}_1$ in the axial direction.

In the moving frame of reference, the liquid at infinity has axial velocity $-\overline{W}_1$, so that $-\overline{W}_1 x_1 = -\overline{W}_1 r\cos\theta$ is added everywhere to the velocity potential ϕ. The integral identity (1.5) is unaffected by this addition to ϕ (which obviously cancels on both sides of the identity), but the two surface integrals on the left-hand side

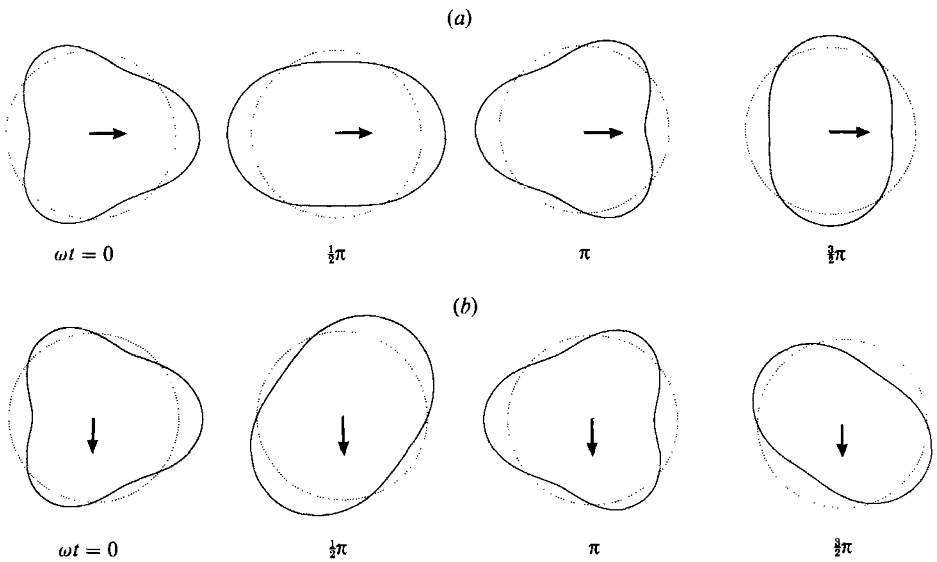

FIGURE 3. (a) Shapes of bubble at quarter-period intervals when modes 2 and 3 are aligned and vibrate in quadrature, so producing maximum propulsion. (b) Shapes of bubbles at quarter-period intervals when mode 2 has axis $\theta' = 54.74°$, mode 3 in quadrature having axis $\theta' = 0$, so that $\lambda = 90°$.

admit different interpretations in the moving frame. The first is $\mathrm{d}C_1/\mathrm{d}t$ as before but now ensured to have zero mean value. The second is the sum of I_1, which remains zero in the absence of external forces, and the integral of $\overline{W}_1 x_1 n_1$ over S, which is $\frac{4}{3}\pi a^3 \overline{W}_1$ to $O(\epsilon^2)$. Hence the argument in §§3 and 4, now referred to the moving frame, shows that

$$W_1' + \overline{W}_1 = \sum_{n=2}^{\infty} \frac{9a}{2n+3} \dot{\epsilon}_n \epsilon_{n+1} + O(\epsilon^3), \tag{6.2}$$

where W_1' is the velocity of the centroid in the moving frame, having zero mean value. Note that in this description ϵ_1 has zero mean value, so remaining unequivocally $O(\epsilon^2)$, and (6.2) remains a uniformly valid second-order approximation for all t. This improved, uniformly valid description can obviously be adapted to self-propulsion developed in any direction.

Relaxation of assumption $\epsilon_0 = O(\epsilon^2)$

With regard to practical examples of parametrically excited shape oscillations, it is desirable to qualify the assumption that in (2.1) ϵ_0 too is $O(\epsilon^2)$. This assumption was made to simplify the presentation of the analysis, but it can be relaxed without much extra complication. In §1 we mentioned the linearized equation for each $\epsilon_n(t)$ derived by Plesset & Mitchell (1956), which equation accounts for the effects of surface tension and for a prescribed time-dependent mean radius $a\{1+\epsilon_0(t)\}$ of the bubble. The frequency σ_n of free vibrations in a mode $n \geqslant 2$ is given by the well known formula $\sigma_n^2 = (n-1)(n+1)(n+2)T/a^3$, where T is the surface-tension coefficient divided by the density of the liquid (Lamb 1932, p. 475); and of course the equation in question reduces to $\ddot{\epsilon}_n + \sigma_n^2 \epsilon_n = 0$ in the case $\epsilon_0 \equiv 0$. When $\epsilon_0(t)$ varies periodically with sufficient amplitude $\hat{\epsilon}_0$ at a frequency 2ω not too far from $2\sigma_n$, as when the bubble pulsates in response to ambient pressure variations at this frequency (e.g. to sound waves with wavelength $\gg a$ in the liquid), the equation has solutions that are oscillatory at frequency ω and grow in amplitude exponentially with t. The growth is eventually arrested by nonlinear effects; and if ω is close enough to σ_n, the eventual amplitude $\hat{\epsilon}_n$ of ϵ_n can in principle be arbitrarily larger than the least $\hat{\epsilon}_0$ needed to induce the parametric excitation. When viscous damping is ignored, the theory indicates that $\hat{\epsilon}_0/\hat{\epsilon}_n \rightarrow 0$ is possible as $\omega \rightarrow \sigma_n$.

The assumption $\epsilon_0 = O(\epsilon^2)$ is thus justified in a narrow range of prospective applications. With allowance for damping, however, and particularly with regard to examples where $\hat{\epsilon}_0$ is large enough for simultaneous excitation of two modes n and $n+1$, the assumption becomes doubtful. We shall not explore the matter fully here, merely noting as follows how our main results are generalized to include the effects of unrestricted ϵ_0.

The preferable course is to suppress ϵ_0 in (2.1) and treat a as a (positive) function of t. Then (2.2) has to be replaced by

$$\phi = -\frac{a^2\dot{a}}{r} - \frac{Aa^4\mu}{r^2} - \sum_{n=2}^{\infty} \frac{\{a^{n+3}\dot{\epsilon}_n + 3a^{n+2}\dot{a}\epsilon_n + O(\epsilon^3)\}P_n(\mu)}{(n+1)\,r^{n+1}}.$$

(Note that this expression for ϕ satisfies the kinematic boundary condition to $O(\epsilon)$, for arbitrary $a(t)$. When it is substituted into the dynamic boundary condition, the coefficient of $P_n(\mu)$ gives the differential equation for $\epsilon_n(t)$ mentioned above.) The calculation of A based on $I_1 = 0$ can hence proceed as in §§2 and 3, leading with the modification included in (6.2) to

$$W_1' + \overline{W}_1 = \sum_{n=2}^{\infty} \frac{9}{2n+3}(a\dot{\epsilon}_n + 2\dot{a}\epsilon_n)\,\epsilon_{n+1} + O(\epsilon^3). \tag{6.3}$$

In this result $a(t)$ is unrestricted. Taking $a = a_0(1+\epsilon_0 \cos 2\omega t)$ and $\epsilon_n, \epsilon_{n+1}$ as specified before (6.1), we obtain in place of (6.1)

$$\overline{W}_1 = \frac{9}{4(2n+3)}\omega a_0\, \hat{\epsilon}_n\, \hat{\epsilon}_{n+1}\{2\cos(\alpha-\beta) - 3\epsilon_0 \cos(\alpha+\beta)\} + O(\epsilon^3). \tag{6.4}$$

With $\alpha = \beta = \frac{1}{2}\pi$ and $\epsilon_0 > 0$, for example, $\overline{W}_1$ is increased above the estimate (6.1) by a factor $1+\frac{3}{2}\epsilon_0$. The propulsive effect is thus possibly reinforced by volume pulsations that excite modes n and $n+1$ parametrically.

Interpretation

The explanation of dancing bubbles as reported by Kornfeld & Suvorov (1944) is already implied, but we finally need to focus the facts available. Generalized as in §5 our theoretical result (6.2), or the more accurate (6.3), shows that self-propulsion generally arises whenever modes n and $n+1$ $(n = 2, 3, \ldots)$ are both excited parametrically. The effect disappears only when the modes are in exact temporal phase. When the interacting modes depart from axial alignment, the vector mean velocity $\overline{\boldsymbol{W}}$ of the bubble's centroid is comparatively little diminished in magnitude but its direction is markedly changed. Thus, drifting of the relative temporal phase of the modes may momentarily arrest the self-propulsion; drifting of their spatial phase may drastically change the direction in which the bubble is propelled.

The simultaneous parametric excitation of spatially distinct modes has been much studied recently in another case, namely surface waves on a liquid layer supported by a vibrating platform (e.g. see Gollub & Meyer 1983; Ciliberto & Gollub 1985). It has been found experimentally that, in particular when the amplitude and frequency 2ω of the excitation are near the intersection of the stability loci respective to two modes, nonlinear competition between the modes can result in either periodic or chaotic changes in their intensity on a long timescale. In fact, a mild form of both temporal and spatial chaos is conspicuous in a simple demonstration which the present authors have often watched. When a liquid layer is vibrated vertically at fairly high frequency, such that many different modes with approximately the same wavenumber can be excited, the wave-pattern changes incessantly without ever exhibiting order, and the wandering cells of the wave-pattern vary erratically in amplitude.

Comparable effects of competition between modes must be expected in the case of bubbles, and the mobility of each interacting mode over the whole of the symmetry group $O(3)$ seems likely to contribute to the chaotic character of possible motions. The effects demonstrated in this paper may propel bubbles along erratic paths as a by-product of independently chaotic interactions between ϵ_n and ϵ_{n+1}; but the probable sensitivity of the interactions to small changes in conditions along any path may itself be a prime cause of chaos. When shape oscillations in modes n and $n+1$ are excited, a bubble acquires propulsion with every direction possible – like a skater on ice holding a rocket, who too may move in an erratic path!

A few experimental observations

To conclude, we introduce a sample of our experimental findings, a full account of which we hope to present later (Ellis & Benjamin 1990). In the experiments high-speed photography was used to record the behaviour of single small bubbles in distilled and degassed water, a depth 197 mm of which was contained in a cylindrical Pyrex beaker with internal diameter 172 mm and wall thickness 3.2 mm. A magnetostrictive ring, of height 25.4 mm, resting on the bottom of the beaker, was driven at a frequency 10 kHz, exciting a radially symmetric acoustic standing wave in the water and beaker. Because this frequency was close to a frequency of resonance for the composite mechanical system, virtually simple-harmonic oscillations of pressure in the water could thus be produced with a fixed spatial distribution and with easily controlled amplitude. (For a detailed discussion of this method of excitation in a related application, see Ellis 1955.) Helium was used to make the bubbles because of its comparatively low solubility in water. The bubbles, typically with radius a about 0.1 mm, were released singly from a pipette at the bottom of the beaker and would rise to become eventually suspended by Bjerknes forces above a central antinode of the standing wave, which was measured to be 46.9 mm below the free surface (i.e. a little further below than a quarter-wavelength of an untrapped wave at frequency 10 kHz in water).

[Note that, for helium bubbles of this size at approximated atmospheric pressure, the frequency 10 kHz is far below resonance in respect of volume pulsations. Variations in volume are therefore in antiphase with simple-harmonic variations in ambient pressure, and so the Bjerknes force on such a bubble is $\alpha \nabla \hat{p}^2$, where α is a positive coefficient depending on a and $\hat{p}$ is the spatially varying pressure amplitude. Thus the force propels the bubble towards the centre of a radially symmetric standing wave; and, at a point between the first antinode and the free surface, it may balance the buoyancy force on the bubble.]

Suspended bubbles were photographed through a telescope by means of microsecond flash illumination. Because the bubbles gradually changed in size due to diffusion of the helium contents into or out of solution, decreasing when the water

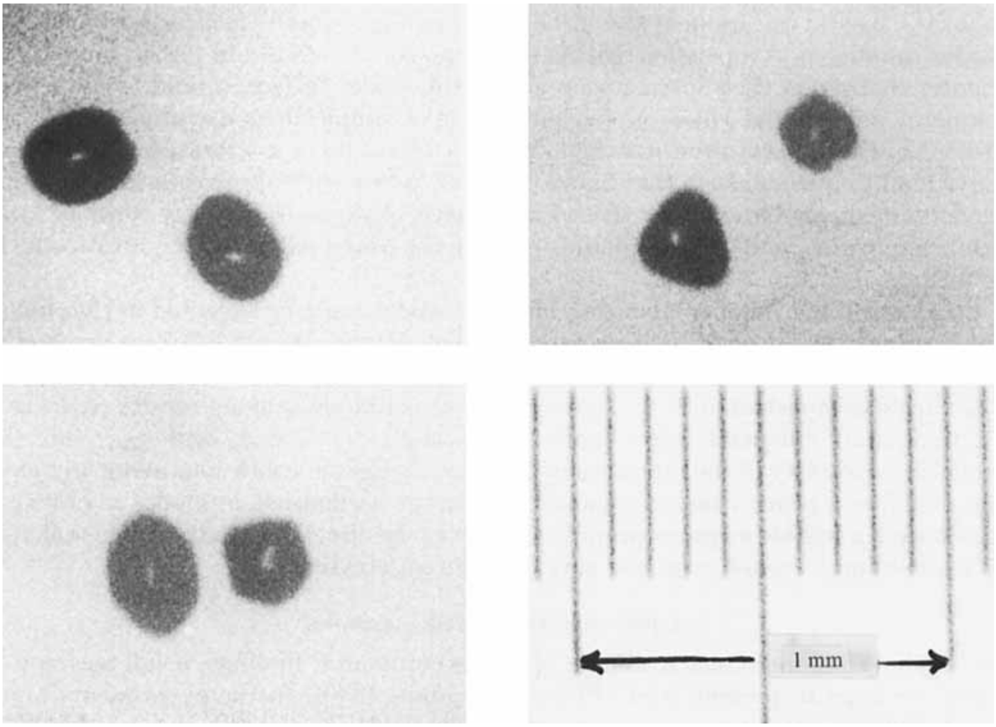

FIGURE 4. Double-exposure flash photographs of vibrating bubbles, the interval between successive exposures being 0.05 s.

was undersaturated or saturated and increasing when it was oversaturated, a variety of parametrically excited asymmetric behaviour was observable in the same bubble. It was found that each of the modes $n = 2, 3, 4, 5, 6$ could be excited, being inducible at more or less minimal pressure amplitude when the size of the bubble radius was such that the normal frequency $\sigma_n/2\pi$ of the mode was close to 5 kHz. Thus, with surface tension taken to be 74 mN/m, the favoured values of a for $n = 2$, 3 and 4 are indicated to be 0.097, 0.144 and 0.189 mm respectively, which values were found to be borne out more or less. Close exploration of this aspect was hampered, however, by the need for the pressure amplitude to be high enough to maintain the suspension of the bubbles. At higher amplitudes (around 0.2 atm. and above), simultaneous excitation of different modes commonly occurred, leading to the propulsion of bubbles in wildly erratic paths through distances typically as much as 10 mm (i.e. hundreds of diameters).

Three photographs of self-propelled bubbles are shown in figure 4. Each photograph is a double exposure spaced at an interval of 0.05 s, which corresponds to 250 periods of the shape oscillations at frequency 5 kHz. The fourth photograph shows a scale immersed in the water at the location of the bubbles; from it the sizes of the bubbles and the distances travelled by them in 0.05 s can be estimated. The first photograph catches two phases of near maximum deformation, spaced by about π, in mode $n = 2$. The direction of propulsion appears to have been about 50° from the major axis of the first, upper left elliptical image, from which fact the calculations in §5 indicate that the propulsion was caused by interaction with shape oscillations in mode $n = 3$, whose axis was directed at about 24° from the axis of mode $n = 2$. The presence of mode $n = 3$ is not directly conspicuous in the photograph; but another sign of its being present is that, unlike the first image, the highlight in the second image is displaced from the centre.

The distance travelled by the bubble in the first photograph was 0.50 mm in 0.05 s, so that its speed was 10 mm/s, and its radius was about 0.13 mm. With this value of a and with allowance that $\theta' = 24°$, the formula (6.1) gives $\overline{W} = 2.20 \times 10^3 \times \epsilon_2 \epsilon_3$ mm/s when $\alpha = \beta$. It may be estimated from the first photograph that ϵ_2 was about 0.08, whence the measured speed would be recovered if $\epsilon_3 = 0.06$ roughly. This value seems reasonable, and a higher value would be predicted if the modes $n = 2$ and $n = 3$ were not exactly out of phase. The theory thus appears to be broadly compatible with the observations.

The second photograph, to the right of the first, plainly demonstrates a propulsive interaction between modes $n = 3$ and $n = 4$. The velocity in a plane perpendicular to the line of sight is about the same as the first case; however, because the second image is smaller and less well in focus than the first, it appears that the bubble was also propelled away from this plane. The image on the right of the third photograph indicates the presence of mode $n = 5$, but the image on the left suggests mode $n = 2$ rather than $n = 4$ as might be expected. There is nevertheless no general reason against mode $n = 2$ being excited as well as a propulsive interaction between modes $n = 4$ and $n = 5$.

We warmly appreciate the privilege of contributing to this volume of the *Journal of Fluid Mechanics* in honour of George Batchelor, to whom both of us are indebted scientifically. One of us (T.B.B.) is particularly indebted for sterling advice and encouragement at an early stage of his career.

REFERENCES

Batchelor, G. K. 1967 *An Introduction to Fluid Dynamics*. Cambridge University Press.

Benjamin, T. B. 1964 Surface effects in non-spherical motions of small cavities. In *Cavitation in Real liquids* (ed. R. Davies), pp. 164–180. Elsevier.

Benjamin, T. B. 1987 Hamiltonian theory for motions of bubbles in an infinite liquid. *J. Fluid Mech.* **181**, 349–379.

Benjamin, T. B. 1989 Note on shape oscillations of bubbles. *J. Fluid Mech.* **203**, 419–424.

Benjamin, T. B. & Strasberg, M. 1958 Excitation of oscillations in the shape of pulsating gas bubbles; theoretical work. (Abstract) *J. Acoust. Soc. Am.* **30**, 697.

Ciliberto, S. & Gollub, J. P. 1985 Chaotic mode competition in parametrically forced surface waves. *J. Fluid Mech.* **158**, 381–398.

Ellis, A. T. 1955 Production of accelerated cavitation damage by an acoustic field in a cylindrical cavity. *J. Acoust. Soc. Am.* **27**, 913–921.

Ellis, A. T. & Benjamin, T. B. 1990 Behaviour of bubbles in liquids subject to intense sound fields. (In preparation.)

Gaines, N. 1932 Magnetostriction oscillator producing intense audible sound and some effects obtained. *Physics* **3**, 209–229.

Gollub, J. P. & Meyer, C. W. 1983 Symmetry-breaking instabilities on a fluid surface. *Physica* D **7**, 153–180.

Hsieh, D.-Y. & Plesset, M. S. 1961 Theory of rectified diffusion of mass into gas bubbles. *J. Acoust. Soc. Am.* **33**, 206–215.

Jeffreys, H. & Jeffreys, B. S. 1956 *Methods of Mathematical Physics*, 3rd edn. Cambridge University Press.

Kochin, N. E., Kibel, I. A. & Roze, N. V. 1964 *Theoretical Hydromechanics*. Interscience.

Kornfeld, M. & Suvorov, L. 1944 On the destructive action of cavitation. *J. Appl. Phys.* **15**, 495–506.

Lamb, H. 1932 *Hydrodynamics*, 6th edn. Cambridge University Press (Dover edition 1945).

Lighthill, M. J. 1978 *Waves in Fluids*. Cambridge University Press.

Milne-Thomson, L. M. 1968 *Theoretical Hydrodynamics*, 5th edn. Macmillan.

Plesset, M. S. & Mitchell, T. P. 1956 On the stability of the spherical shape of a vapor cavity in a liquid. *Q. Appl. Maths* **13**, 419–430.

Saffman, P. G. 1967 The self-propulsion of a deformable body in a perfect fluid. *J. Fluid Mech.* **28**, 385–389.

Strasberg, M. & Benjamin, T. B. 1958 Excitation of oscillations in the shape of pulsating gas bubbles; experimental work. (Abstract) *J. Acoust. Soc. Am.* **30**, 697.

Whittaker, E. T. & Watson, G. N. 1927 *Modern Analysis*, 4th edn. Cambridge University Press.